LA-UR-98- 2183

Approved for public release; distribution is unlimited.

Title: MOLECULAR DYNAMICS SIMULATIONS AND THERMOCHEMISTRY OF REACTIVE ION ETCHING OF SILICON BY CHLORINE, CHLORINE DIMER, BROMINE, AND BROMINE DIMER CATIONS

CONF-980430--

Author(s): Steven M. Valone, MST-8
David E. Hanson, T-12
Joel D. Kress, T-12

Submitted to: Proceedings of the Modeling and Simulation of Microsystems, Semiconductors, Sensors and Actuators, 1998 Conference. Santa Clara CA, 4-6 April, 1998.

DISTRIBUTION OF THIS DOCUMENT IS UNLIMITED

MASTER

Los Alamos
NATIONAL LABORATORY

Los Alamos National Laboratory, an affirmative action/equal opportunity employer, is operated by the University of California for the U.S. Department of Energy under contract W-7405-ENG-36. By acceptance of this article, the publisher recognizes that the U.S. Government retains a nonexclusive, royalty-free license to publish or reproduce the published form of this contribution, or to allow others to do so, for U.S. Government purposes. Los Alamos National Laboratory requests that the publisher identify this article as work performed under the auspices of the U.S. Department of Energy. The Los Alamos National Laboratory strongly supports academic freedom and a researcher's right to publish; as an institution, however, the Laboratory does not endorse the viewpoint of a publication or guarantee its technical correctness.

Form 836 (10/96)

DISCLAIMER

This report was prepared as an account of work sponsored by an agency of the United States Government. Neither the United States Government nor any agency thereof, nor any of their employees, makes any warranty, express or implied, or assumes any legal liability or responsibility for the accuracy, completeness, or usefulness of any information, apparatus, product, or process disclosed, or represents that its use would not infringe privately owned rights. Reference herein to any specific commercial product, process, or service by trade name, trademark, manufacturer, or otherwise does not necessarily constitute or imply its endorsement, recommendation, or favoring by the United States Government or any agency thereof. The views and opinions of authors expressed herein do not necessarily state or reflect those of the United States Government or any agency thereof.

DISCLAIMER

Portions of this document may be illegible in electronic image products. Images are produced from the best available original document.

Molecular Dynamics (MD) Simulations and Thermochemistry of Reactive Ion Etching (RIE) of Silicon by Cl, Cl_2, Br and Br_2 Cations[†]

Steven M. Valone,[1] David E. Hanson[2], and Joel D. Kress[2]
[1] Materials Science and Technology Division
[2] Theoretical Division
Los Alamos National Laboratory, Los Alamos, New Mexico USA, 87545

The difficulty in understanding plasma-surface interactions stems from a combination of physical complexity and an experimental environment that is difficult to interrogate. Because plasma-surface interactions have proven so very difficult to characterize experimentally, considerable effort has been expended to model RIE at an atomistic scale using as fundamental inputs the best available experimental data supplemented with *ab initio* electronic structure calculations of bond energies. From this rationale has come MD simulations of Si RIE by chlorine-containing plasmas based on atomistic models of interactions between plasma and surface, producing detailed yield, product distribution, chlorosilyl layer stoichiometry and surface roughness dependencies on impact energy and angle. These simulations have begun the process of understanding the relative contributions of physical collisions versus chemical reactions, sources of surface roughness in real devices, and feedback to feature and reactor scale models

Previous MD simulations of Si RIE with Cl^+ and Cl_2^+ using a form of the Stillinger-Weber potential [1-2] due to Feil (SW/Feil) [3] have been reported by Feil et al. [3-4], Barone and Graves [5-8] and Hanson et al. [9] for the 15-200 eV range of ion impact energies. Within the wide scatter in experimental results, the yields inferred from their MD simulations were consistent with the then-available experimental values from a variety of reactor [10] and ion beam [11-14] results (Fig. 1).

The more recent results of Balooch et al. [11], Layadi et al. [12] and Chang and Sawin [13-14] suggest that the MD yields are too low at least in the 30-75 eV range and perhaps for all energies. Here we will examine how at least some of this deficiency can be explained through an improvement in the interatomic potential model used in the MD simulations.

The essence of this improvement derives from recognizing that the Si-Si bond energies vary with local chemical environment. That is, as the number of nearest neighbors of one Si atom changes, the bond dissociation energy with another Si atom, which is one of its neighbors, changes. This trend in bond dissociation energies is reflected in Table 1.

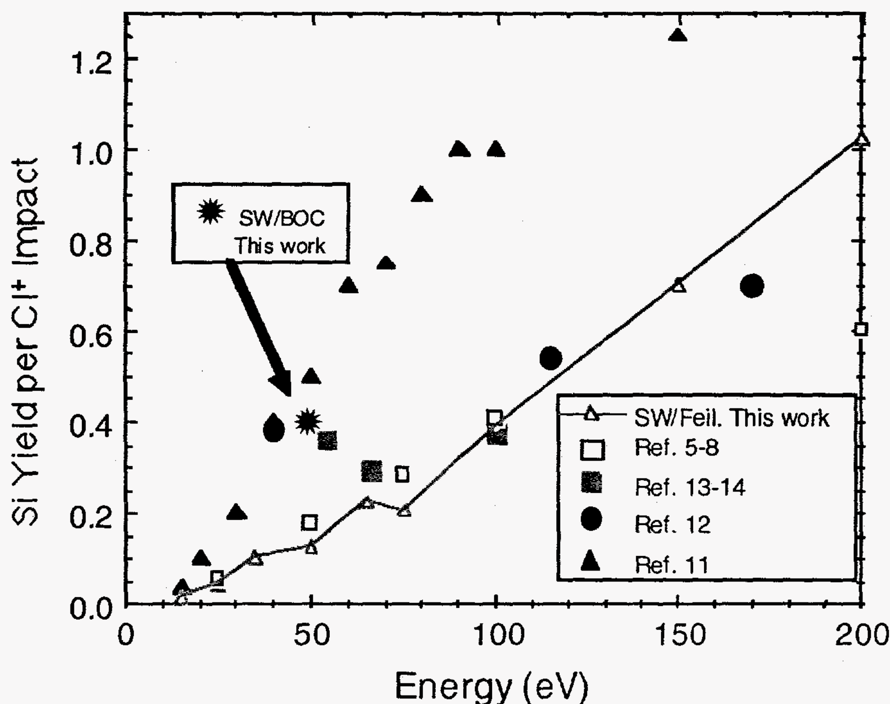

Figure 1. Si yield per Cl^+ impact at indicated ion energy. Some simulations agree well with experimental results even to fairly low energies. More recent experiments suggest that the yields are higher particularly at lower impact energies, prompting a modification of the atomistic model. See Refs. [5-14].

Table 1. Si-Si bond dissociation energies in eV for $(SiCl_n)_2$ molecules. The "AM" row represents MP4-BAC values [15] which are first principles calculations which have been systematically corrected by calibrating with experimental data. Zero point energy corrections are included.

n →	0	1	2	3
AM	3.2	1.8	1.0	3.5

Table 2. Relative Si-Si bond strengths for $(SiH_3)_n Si — SiCl_m$ (eV) from Boehm et al. [17] normalized to the bulk Si value, 2.17 eV/atom [18]. The (0,0) value of 1.06 is for the Si_2 molecule.

n → m ↓	0	1	2	3
0	1.06	0.70	0.58	0.86
1	0.70	0.64	0.40	0.84
2	0.58	0.40	0.36	0.52
3	0.86	0.84	0.52	1.10

The remainder of the paper consists of a discussion of the bond-order correction (BOC) and the MD simulation methodology, product distributions for Si-Cl plasma etch, angular dependence, characterization of the chlorosilyl layer, and a brief discussion about the trends expected in Br etch based on thermodynamic considerations.

POTENTIAL ENERGY SURFACE

The BOC modification to the SW/Feil potential includes a four-body term to account for the effect of neighboring Cl atoms on the strength of the Si — Si bond. The strength of the Si — Si bond is corrected by a factor that depends on the number and type of the other bonds. This potential we denote by SW/BOC. A similar BOC potential was introduced by Brenner [16] to account for π bonding in hydrocarbon molecules. Using fourth order Moller-Plesset perturbation theory (MP4) with a semi-empirical bond additivity correction (BAC), Allendorf and Melius [15] found that the Si — Si bond strength in a $Cl_2Si — SiCl_2$ molecule is only about one half of that for ClSi — SiCl, and that of $Cl_3Si — SiCl_3$ is about a factor of two larger. See Table 1. Intuition suggests that the same effect should obtain if the Cl atoms bound to one of the Si atoms are replaced by Si atoms. This is indeed the case. *Ab initio* electronic structure (gradient-corrected density functional theory, GC-DFT) calculations [17] for this system are shown in Table 2 after being normalized to the value for the bulk Si — Si bond strength of 2.17 eV/atom [18]. The all-electron GC-DFT results are consistent with the more computationally demanding MP4-BAC results [15] for molecules containing Si, Cl and H. Although the minimum bond strength for $(SiH_3)_2Si — SiCl_2$ is not as low as the MP4-BAC value for $Cl_2Si — SiCl_2$, the Si — Si bond strength for either $(SiH_3)_nSi — SiCl$ or $(SiH_3)_nSi — SiCl_2$ (n = 1 - 3) is less than the Si — Si bulk value. In MD simulations of RIE, this could have a significant effect on both the yield and the stoichiometry of the desorbed material.

Other details about the SW/Feil potential and our simulation methodology can be found in Refs. [1,2 and 9]. We emphasize that this is a preliminary version of a SW/BOC potential, and the MD simulation results should be regarded as such.

MD SIMULATION METHODOLOGY

The MD simulation cell, shown in Fig. 2 after 432 100-eV Cl atom impacts, was comprised initially of a 12 x 12 x 7 (x,y,z) atom cell for a total of 1008 Si atoms with periodic boundary conditions imposed along the x and y axis (period = 32.58 Å) and a free, unreconstructed (001) surface

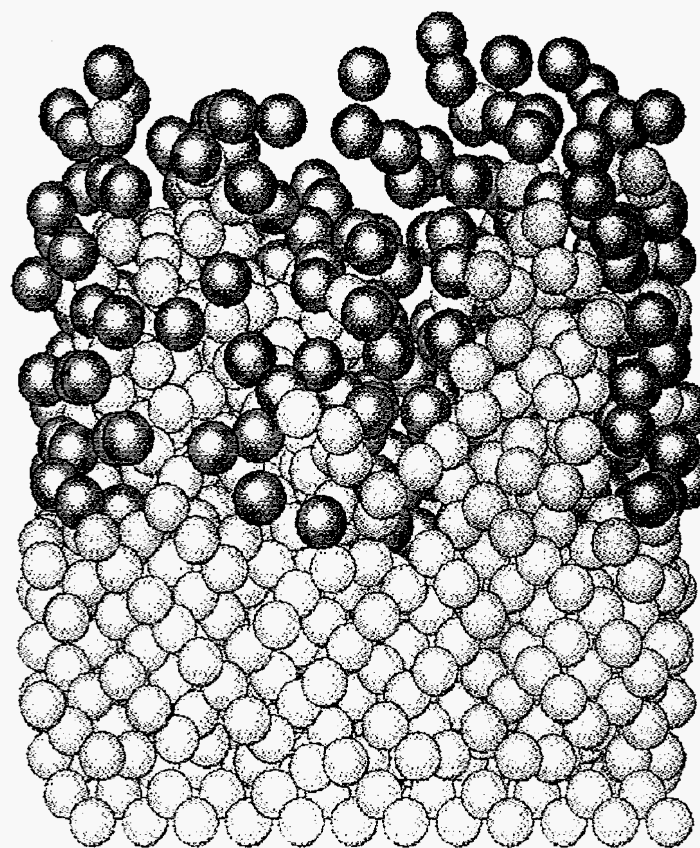

Figure 2. Surface morphology of a chlorosilyl layer in Cl_2 etch plasma on (100) Si surface. The darker balls represent adsorbed Cl atoms and the lighter ones Si atoms. See discussion above on periodicity. Result due to 432 (6 ML) impacts at 100 eV. Note development of nanofissures. The cell size is approximately 33 X 33 $Å^2$ in the in-plane directions.

normal to the z axis. The topmost layer contained 72 atoms (1 ML) and had a surface area of 1061 $Å^2$. The bottom two layers of the cell, 144 atoms, were rigidly fixed at all times. The initial temperature of the cell was 300 K. For the first 40 fs of each impact event, when individual atom velocities are

highest, a time step of 0.2 fs was used, and, for the remaining 460 fs, the time step was 0.8 fs, comparable to the value used by Barone and Graves [5,6] of 0.7 fs. Please see Ref. 9 for additional details.

We simulated etching by Cl^+ only rather than by both Cl^+ and Cl_2^+ for two reasons: The previous simulation work most relevant for comparison [3-8] used Cl^+ and the predominant species in plasma reactors is observed through Langmuir probe and optical emission to be Cl^+ [19].

A single Cl^+ ion, assumed to be neutralized by a fast Auger process [20] before interacting with the surface, was directed normal to the (001) surface at the desired energy (15 eV $\leq$ E $\leq$ 200 eV) at randomly chosen x,y coordinates. In this paper, all references to "impact ion" are to be interpreted as a neutral atom. Interatomic forces were computed from analytic expressions of derivatives of the two and three body potentials and the equations of motion were integrated using the velocity-Verlet method [21].

Our desorption algorithm required candidate molecules to satisfy the following criteria. The z coordinate value of the atom being considered must be greater than some predetermined value (set by visually inspecting the simulation cell at the beginning of a series of impacts), and all of the atom's bonded neighbors must also be above this z plane. At the end of each series of ion impacts, usually 72 (1 ML), the cell was visually inspected and any desorbed molecules not detected by the desorption algorithm due to the complex morphology of the surface were removed from the cell. The initial state for subsequent ion impacts used the final state of the previous impact. We believe that this procedure allows desorbed molecules not yet detected by the desorption algorithm, or weakly bound surface moieties, to be correctly counted.

PLASMA ETCH PRODUCT DISTRIBUTIONS

In Figs. (3a and 3b) we show the etch product distributions for 50 and 100 eV impact energies for both the SW/Feil (gray) and the new SW/BOC (black) potentials. At either energy, the SW/BOC potential generates a higher fraction of $SiCl_2$ molecules compared to the SW/Feil potential. For either potential, the dominant product at the lower energy is $SiCl_2$, while the dominant product at the higher energy is SiCl and the distribution is broader. A longstanding debate within the plasma etch community revolves around the relative roles of physical versus chemical etch processes. Clearly there is no sharp distinction between the two processes, but generally one means that a physical process results in removal of some material due to the direct impact of a plasma ion with the surface, while a chemical process involves some sort of mediated energy transfer between the impact site and the desorption site. For instance, for physical etch, Barone and Graves [5-8] use the criterion that the desorption product contains the incident ion. However, other criteria are also possible. At higher energies the broader distribution and the dominance of a nonequilibrium product distribution (see the bond strengths in Table 1) is consistent with the intuitive notion that physical processes play a larger role as impact energy increases.

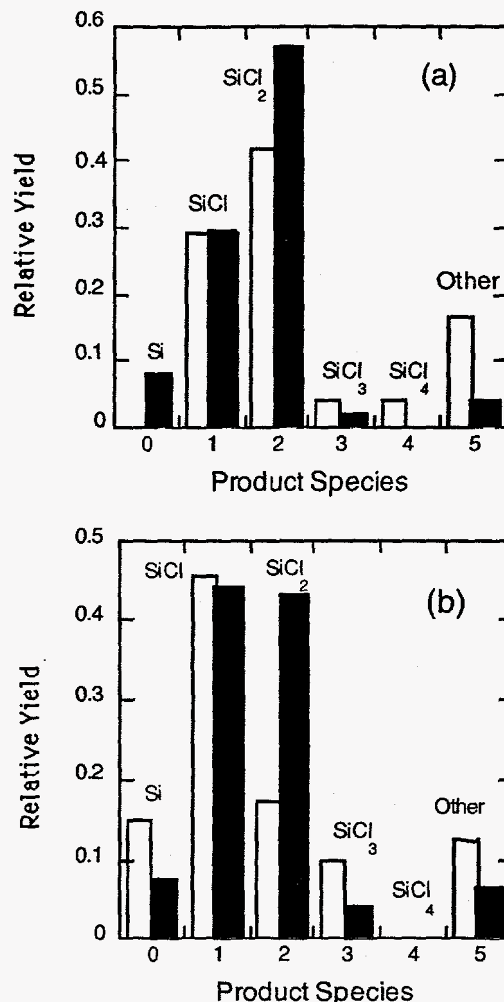

Figure 3. Etch product distributions at (a) 50 eV and (b) 100 eV Cl impact energies for the SW/Feil (gray) and SW/BOC (black) potentials. Product distributions are broader at the higher energy for either potential. However, the SW/BOC potential allows substantially higher SiCl and $SiCl_2$ production at both energies. Note that the yield scales are slightly different in the two graphs.

CHARACTERIZATION OF THE CHLOROSILYL LAYER

Referring again to Fig. (2), several features of the chlorosilyl layer are of interest. One is the positions of the surface Si atoms relative to their ideal bulk positions. We find that for all of the apparent surface roughening, most of the Si surface atoms are relatively unperturbed with respect to bond distances. This can be quantified in the radial distribution function (Fig. 4) where the average number of Si neighbors of a surface Si is 2.7 and the average number of Cl neighbors for an Si atom is 1.2. As further support of this claim, the triangular symbols denote the bulk Si positions which all fall

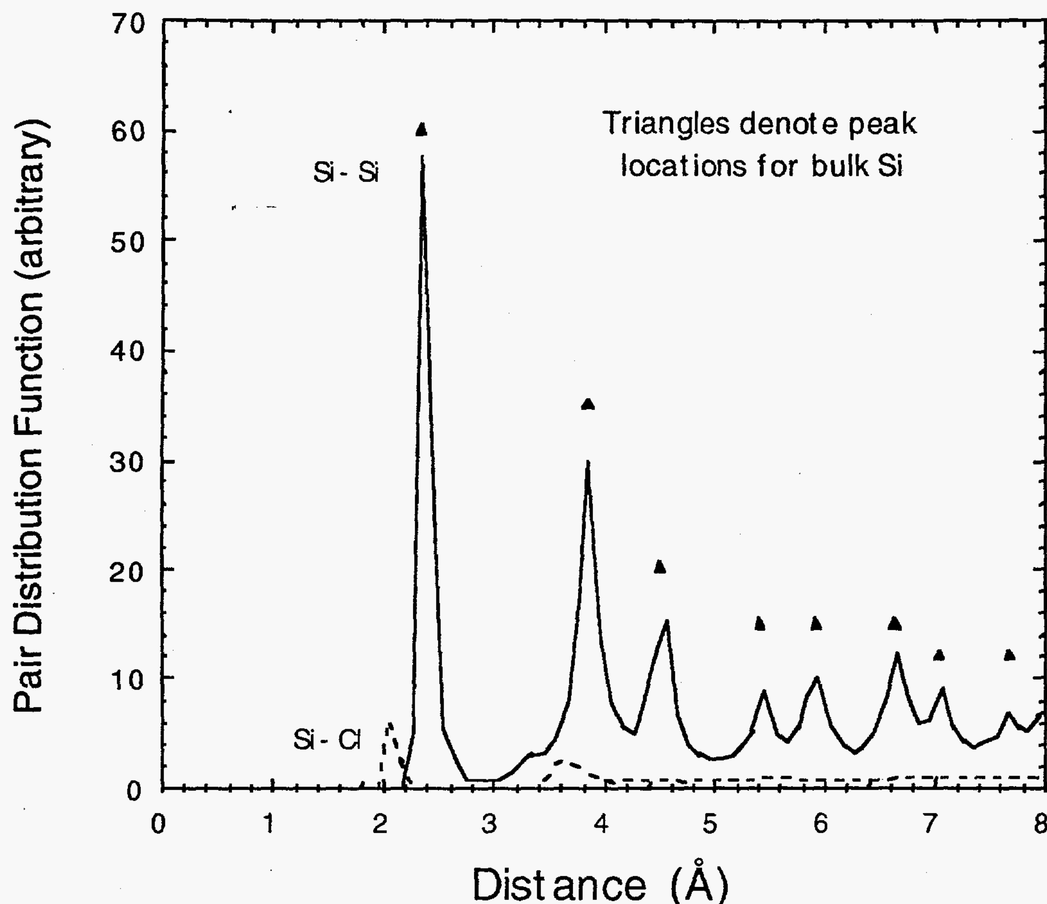

Figure 4. Pairs Distribution functions for Si-Si and Si-Cl in arbitrary units. The triangles mark the positions of the Si atoms in their ideal bulk arrangement.

close to the peaks positions in the Si-Si pair distributions function for the chlorosilyl layer.At an even greater level of detail, we can compute the relative ratios of Si having various numbers of Cl neighbors. Normalizing to SiCl (i.e., surface Si with one Cl neighbor), for the SW/BOC potential, we find the ratios 1.00:0.32:0.04 for $SiCl:SiCl_2:SiCl_3$. Analogously X-ray photoelectron spectroscopy (XPS) data from Layadi et al. [23] gives the values 1.00:0.34:0.09. The MD simulations of Barone and Graves [5-8] with the SW/Feil potential find, as reported in Ref. 23, 1.00:0.14:0.01. This is further evidence that the bond-order correction described earlier is essential for quantifying Si etch rates from MD simulations.

The RMS surface roughness of 6 ± 0.5 Å, extracted from the present MD simulations, is comparable to that found by atomic force microscopy (AFM) from Sung and Pang (1.6-6.4 Å) [24]. Moreover the peak-to-peak extremes are often on the order of 20 Å. This depth is comparable to that seen in contemporary devices. However some caution is necessary. The size of the features is comparable to the size of the simulation cell. For a system with periodic boundary conditions this is very undesirable. One really needs to make the simulation cell size twice that of any feature that one seriously wishes to examine. Furthermore, the timescale over which the chlorosilyl layer relaxes is expected to be orders of magnitude longer than the timescale for the etch impacts. These long timescales are very difficult for MD simulations to reach. For these reason, the details of the layer structure must be regarded as uncertain. Nevertheless the depth of some of the features, as well as the agreement between both the XPS and AFM data and the simulations, is suggestive as to a possible source of nanometer-scale roughness in trench and via device features.

Yield Dependence on Impact Angle

The angular dependence in the yield at a fixed energy, Fig. 5, features a peak in the 50-70° range for 100 eV impact energies as show in Fig. 5. The absence of strong angular dependence between 0 and 40° is supported by measurements from Chang and Sawin [13-14]. The reason for this may be the previously discussed surface roughness which effectively averages the incidence angles over a broad range until the angles become nearly glancing.

The values of the MD simulation yields and angular dependencies were incorporated into a trench profile etch simulation by Hoekstra et al. [25] using a Monte Carlo algorithm and compared with a simulated profile resulting from experimental etch rates and angular dependences. The main difference between the two stems from the difference in

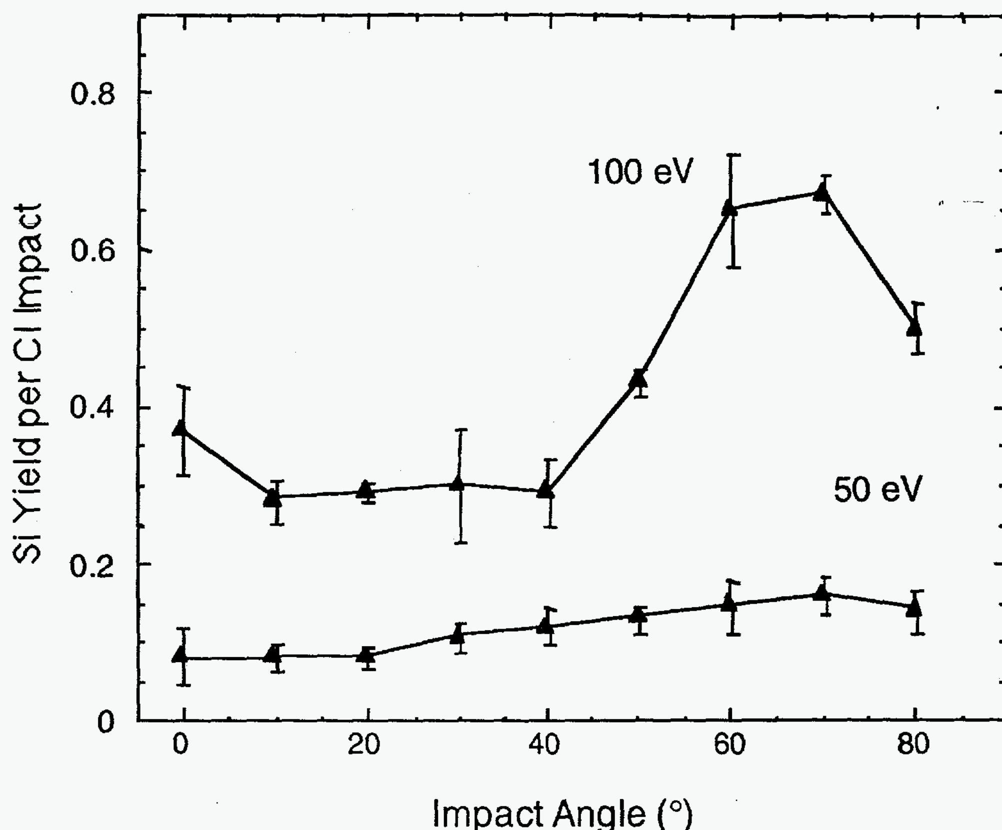

Figure 5. Variation in yield with respect to impact angle with relative to normal incidence, that is the <100> direction. The greatest sensitivity appears at the more glancing angles.

etch rates rather than from differences in the angular distributions. Overall the agreement is good and suggests that MD simulations on systems for which there is less experimental information available can provide useful inputs for profile simulation.

THERMOCHEMICAL IMPLICATIONS FOR BR ETCH RATES

Based on the similarity in Si-Si bond strengths for the Si-Br versus the Si-Cl systems (Table 3), one would expect the etch rates to comparable. Experimentally, this is the case [27] where most of the difference in etch rates is ascribed to differences in the ion fluence for Br^+ versus Cl^+ under comparable plasma conditions. The per-halogen etch rate for Br^+ may in fact be slightly higher than Cl^+. The calculations demonstrate that the Si-Si bond strength is little influenced by the substitution of Br for Cl. Indeed SiBr and $SiBr_2$ surface species do predominate and these same species are observed as etch products [28], albeit that the mass spectrometry data is much less extensive compared to the chlorosilyl system.

As for surface morphology there are several possible influences that will need to be explored. First is the difference in bond distances, the Si-Br bond distance being about 0.1 Å longer. One expects this to increase steric interference among adsorbed Br, reducing the surface coverage of Br relative to Cl saturation coverage. In addition one would expect steric effects to favor SiBr and $SiBr_2$ surface concentrations even more than for the chlorinated case [27]. Finally this bond length distance could be expected to reduce both the penetration of Br^+ and diffusion of surface Br into the lattice leading to lower film stress in the halosilyl layer and hence less roughness.

Table 3. Si-Si bond dissociation energies in eV for both $(SiCl_n)_2$ (upper) and $(SiBr_n)_2$ (lower) molecules. For the chlorinated molecules, the "AM" is the same as in Table 1. The BLYP row represents values computed by an unrestricted Becke-3, Lee-Yang-Parr density functional method using a 6-311G** basis [26]. For these values the 1-2 kcal/mole zero point energy correction is not included.

$(SiCl_n)_2 \rightarrow 2\ SiCl_n$

n →	0	1	2	3
AM	3.2	1.8	1.0	3.5
BLYP	2.8	1.1	0.4	2.9

$(SiBr_n)_2 \rightarrow 2\ SiBr_n$

n →	0	1	2	3
experiment	X	X	X	X
BLYP	2.9	1.4	0.5	2.4

Similarly the greater mass of Br favors less surface penetration both from diffusional and ion impingement perspectives. Both of these would favor lower RMS roughness and smaller extremes in roughness feature sizes. In addition, the Si-Br bond energies are lower by about 0.8eV per bond compared to the chloro-analogs, 4.0 vs 4.8 eV [29], again facilitating formation of unsaturated Si surface species and reducing the diffusional driving force.

Finally the etch rate sensitivity to dopant levels is more pronounced for Br etch than for Cl etch [30]. This is consistent with the increased lability of the valence electrons in Br compared to Cl. At room temperature and high doping levels, atomic Br does not etch Si whereas the etch rate is appreciable for Cl atoms.

CONCLUSIONS

Simulations of Cl plasma etch of Si surfaces with MD techniques agree reasonably well with the available experimental information on yields and surface morphologies. This information has been supplied to a Monte Carlo etch profile [25] resulting in substantial agreement with comparable inputs provided through controlled experiments. To the extent that more recent measurements of etch rates are more reliable than older ones, preliminary MD simulations using bond-order corrections to the atomic interactions between neighboring Si atoms on the surface improves agreement with experiment through an increase in etch rate and improved agreement with XPS measurements of surface stoichiometry.

Thermochemical and geometric analysis of small Si-Br molecules is consistent with the current notions of the effects of including brominated species in etchant gases.

† Work performed under the auspices of the US Department of Energy under Contract W-7405-ENG-36 with the University of California and supported by a Cooperative Research and Development Agreement between the US Department of Energy and the Semiconductor Research Corporation.

REFERENCES

1. F. Stillinger and T. Weber, *J. Chem. Phys.* **88**, 5123 (1988).
2. F. Stillinger and T. Weber, *Phys. Rev. Lett.* **62**, 2144 (1989).
3. H. Feil, J. Dieleman, and B. Garrison, *J. Appl. Phys.* **74**, 1303 (1993).
4. H. Feil, *Phys. Rev. Lett.* **74**, 1879 (1995).
5. M. E. Barone and D. B. Graves, *J. Appl. Phys.* **77**, 1263 (1995).
6. M. E. Barone and D. B. Graves, *J. Appl. Phys.* **78**, 6604 (1995).
7. M. E. Barone, T. O. Robinson, and D. B. Graves, *IEEE Transactions on Plasma Science* **24**, 77 (1996).
8. M. E. Barone and D. B. Graves, *Plasma Sources Science & Technology* **5**, 187 (1996).
9. D. E. Hanson, A. F. Voter, and J. D. Kress, *J. Appl. Phys.* **82**, 3552 (1997).
10. I. P. Herman, V. M. Donnelly, C. C. Cheng, and K. V. Guinn, *Jpn. J. Appl. Phys.* **35**, 2410 (1996).
11. M. Balooch, M. Moalem, Wei-E. Wang, and A. Hamza, *J. Vac. Sci. Technol. A* **14**, 229 (1996).
12. N. Layadi, V. M. Donnelly, J. T. C. Lee, and F. P. Klemens, *J. Vac. Sci. Technol. A* **15**, 604 (1997).
13. J. P. Chang and H. H. Sawin, *J. Vac. Sci. Technol. A* **15**, 610 (1997).
14. J. P. Chang, (Personal communication, 1997).
15. M. Allendorf and C. Melius, *J. Phys. Chem.* **97**, 720 (1993).
16. D. W. Brenner, *Phys. Rev. B* **42**, 9458 (1990).
17. R. C. Boehm, J. D. Kress, R. L. Martin, and P. J. Hay, *J. Computat. Chem. 19*, 2075 (1997).
18. F. Stillinger and T. Weber, *Phys. Rev. B* **31**, 5262 (1985).
19. E. Meeks, J. Shon, Y. Ra, and P. Jones, *J. Vac. Sci. A* **13**, 2884 (1995); V. M. Donnelly, *J. Vac. Sci. Technol. A* **14**, 1076 (1996); J. Y. Choe, I. V. M. Donnelly, J. T. C. Lee, and F. P. Klemens, *J. Vac. Sci. Technol. A* **15**, 3024 (1997).
20. S. Kasi and J. Rabalais, *Radiation Effects and Defects in Solids*, **112**, 119 (1990).
21. W. C. Swope, H. C. Anderson, P. H. Berens, and K. R. Wilson, *J. Chem. Phys.* **76**, 637 (1982).
22. H. J. C. Berendsen, J. P. M. Postma, W. F. Van Gunsteren, A. D. Nola, and J. R. Haak, *J. Chem. Phys.* **81**, 3684 (1984).
23. N. Layadi, V. M. Donnelly, and J. T. C. Lee, *J. Appl. Phys.* **81**, 6738 (1997).
24. K. Sung and S. Pang, *Jpn. J. Appl. Phys.* **33**, 7112 (1994).
25. R. J. Hoekstra, M. J. Grapperhaus and M. J. Kushner, *J. Vac. Sci. Technol. A* **15**, 1913 (1997).
26. M. J. Frisch, G. W. Trucks, H. B. Schlegel, P. M. W. Gill, B. G. Johnson, M. A. Robb, J. R. Cheeseman, T. A. Keith, G. A. Petersson, J. A. Montgomery, K. Raghavachari, M. A. Al-Laham, V. G. Zakrzewshi, J. V. Ortiz, J. B. Foresman, J. Cioslowski, B. B. Stefanov, A. Nanaynkkara, M. Challacombe, C. Y. Peng, P. Y. Ayala, W. Chem, M. W. Wong, L. J. Andres, E. S. Replogle, R. Gomperts, R. L. Martin, D. J. Fox, J. S. Binkley, D. J. Defrees, J. Baker, J. P. Stewart, M. Head-Gordon, C. Gonzalez, and J. A. Pople, *GAUSSIAN-94 (Revision A.1)*, Gaussian Inc., Pittsburgh, PA, 1995.
27. C. C. Cheng, K. V. Guinn, and V. M. Donnelly, *J. Vac. Sci. B* **14**, 85 (1996).
28. G. C. Tyrrell, I. W. Boyd, and R. B. Jackman, *Surf. Sci.* **43**, 439 (1989).
29. JANAF Thermochemical Tables, 1992 supplement *J. Phys. Chem. Ref. Data*, **11**, No. 3 (1982).
30. Z. H. Walker and E. A. Ogryzlo, *J. Appl. Phys.* **69**, 2635 (1991).